

The Transient Modeling of Single-Bubble Nucleate Boiling in a Sub-Cooled Liquid Using an ALE Moving Mesh

Christopher J. Forster, Marc K. Smith*

School of Mechanical Engineering, Georgia Institute of Technology

*Corresponding author: 771 Ferst Drive NW, Atlanta, GA 30332-0405, marc.smith@me.gatech.edu

Abstract: Power electronics dissipate large amounts of power in a small package. This creates the necessity for cooling technologies capable of high heat fluxes at or below the operating temperature limits of these devices. Boiling heat transfer is an effective way of handling this waste heat removal while limiting the peak temperature of the device. However, heat transfer for pool boiling on a flat plate is limited by a critical heat flux (CHF), which is typically near 125 W/cm^2 for water at standard pressure. The exact value of the CHF depends on many parameters, including heater geometry, surface material, and surface oxidation levels that affect the liquid-vapor contact angle. In particular, the contact angle plays a significant role in vapor-bubble spreading and the onset of CHF. In this work, a high-fidelity numerical model is used to investigate pool boiling with a single bubble in an effort to increase CHF. The model uses an Arbitrary Lagrangian-Eulerian (ALE) moving mesh to directly track the interface. This sharp interface model also offers a simple means to apply the appropriate boundary conditions on the liquid-vapor interface for surface tension and heat transfer with phase change. However, the disadvantage of the ALE method is its difficulty in dealing with changes in topology, such as bubble pinch-off. This paper investigates the evolution of a single bubble going through growth, pinch-off, and condensation while rising due to buoyancy forces in a sub-cooled liquid. Phase change is modeled on the evolving liquid-vapor interface by considering changes in enthalpy and heat fluxes at the interface. A comparison of the ALE model is made with the same single-bubble system computed with a level-set interface tracking formulation.

Keywords: ALE, moving mesh, pinch-off, surface tension, dynamic contact line, nucleate boiling, heat transfer, phase-change, level-set

1. Introduction

In modeling boiling heat transfer near a flat, heated, horizontal surface, the details of the bubbles' liquid-gas interface evolution in time are important in the determination of the critical heat flux. The CHF is crucial for most cooling applications since there is a sudden, large jump in temperature as the boiling transitions from nucleate to film. For electronics cooling, exceeding the CHF will likely lead to the device exceeding design temperatures and failure. The transition to film boiling can be shown on the boiling curve as moving from the CHF local maximum heat flux over to the right-hand, film boiling portion of the curve [1]. It is important to note the transition occurs rapidly and causes a large increase in surface temperature. A qualitative boiling curve is shown in Figure 1.

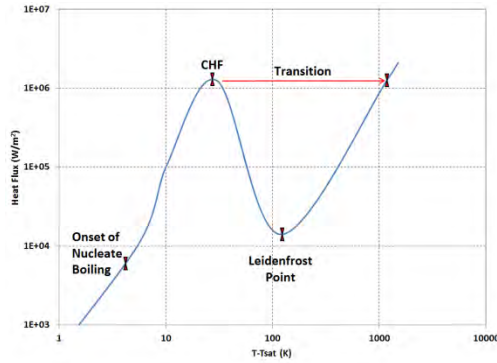


Figure 1. Transition from nucleate to film boiling.

Two models are presented here – an Arbitrary Lagrangian-Eulerian (ALE) and a level-set model. The ALE model allows for more detail in the dynamics of a single vapor bubble, while the level-set model is capable of, and more practical for, modeling multiple vapor bubbles and their bubble-bubble and bubble-wall interactions. Modeling of a single bubble allows for insight into the critical parameters that control bubble growth, departure frequency and size, and bubble spreading, which can lead to earlier onset of the CHF. With this information, the level-set model can then be used to optimize

heater configurations in more practical and complicated cooling applications.

2. Use of COMSOL Multiphysics

2.1 Initial Model Geometry, Initial Conditions, and Boundary Conditions

The bubble begins as a spherical-cap, attached bubble at the bottom of the tank. The initial configuration is shown in Figure 2. The gravity force and heat flux are ramped in over relatively short time scales, 0.05s and 0.1s, respectively. This allows the solver to start more easily, and it allows condensation to be more directly observable before the heat flux input to the bottom of the tank has been fully ramped in. The temperature profile is initially linearly varied from saturation temperature at the hot surface to a sub-cooled temperature at the upper boundary. The amount of sub-cooling can be adjusted, but for this model it is set at 5K, which is reasonable for boiling experiments. The initial velocity field is zero, and the initial pressure field is uniform over each subdomain, with the bubble pressure increased by the Laplace pressure jump. This pressure field is appropriate for zero initial gravity, before gravity is ramped in, and the equilibrium, spherical-cap bubble shape. The model is axisymmetric.

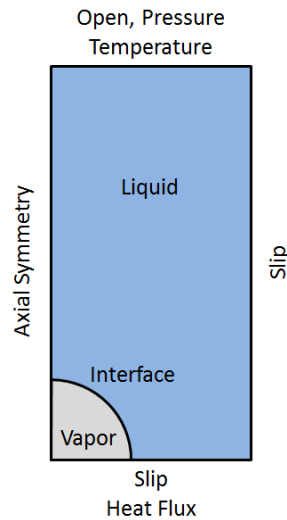


Figure 2. Initial model configuration.

The hydrodynamic boundary conditions will be listed first. The hot plate is modeled as a slip boundary with a fixed contact angle, but each

domain can be set to slip or no-slip independently. Future models may incorporate a contact line mobility model to more accurately capture the contact line dynamics, but for now the two extremes of slip and no-slip are easily modeled. The upper tank boundary is set to zero gage pressure. The right-hand tank wall is set to a slip boundary condition. The vapor-liquid interface enforces a no-slip condition for the tangential velocity component. The normal velocity component accounts for the divergence due to vaporization occurring at the interface. The Young-Laplace normal stress jump is modeled. The vapor recoil pressure can be included, but it was chosen to be neglected in this model. The inclusion of vapor recoil pressure makes the model more unstable, and for lower heat inputs, the vapor recoil pressure is negligible. Vapor recoil pressures were observed to be on the order of 1 Pa while pressure from surface tension is approximately 50 Pa. The vapor recoil effect may be more significant at higher heat inputs.

In each thermal domain, the interface is required to remain at the saturation temperature, which is prescribed to be 373.15K to represent boiling at standard pressure. The saturation temperature can be a function of pressure, but the slight variations in saturation temperature due to pressure variations are neglected here. The energy balance at the interface is maintained by the rate of vaporization or condensation. The heat fluxes are calculated on each side of the interface and the difference determines the rate of vaporization or condensation. The hot plate has a heat flux input prescribed to be 0.2 W/cm² under the vapor bubble and 20 W/cm² everywhere else. This choice is somewhat arbitrary, and the reason behind choosing a non-uniform heat flux is discussed in the results section. The model can be modified to include another domain for the heat transfer model of the solid heater plate to determine the distribution of heat between the bubble and the surrounding liquid. This paper is focused on presenting the interface conditions and modeling of the phase-change, so the additional domain for the heater plate is omitted for clarity. The right-hand side of the tank is modeled as thermally-insulated. The upper tank boundary is held at the saturation temperature minus the amount of sub-cooling, which is 368.15K for this model.

2.2 Pinch-off Transition

Leading up to pinch-off the ALE model is run with remeshing periodically to maintain mesh quality. The pinch-off point is chosen near the minimum neck radius for this simulation. A reasonable gap height is chosen between the attached and pinched bubble to prevent creating excessively small elements in the pinched region. The final geometry of the attached bubble simulation is exported to Matlab as an array of points with the pinch-off points inserted. The boundary points are spline-fit with constraints on end-point tangency. The geometry is imported back into Comsol and boundary conditions are transferred from the previous geometry. The number of fluid domains increases from two to three domains. Since a finite amount of time occurs during pinch-off, which is not modeled here, post-pinch-off velocity, pressure, and temperature fields were estimated in order to continue the simulation. These estimated initial conditions after pinch-off are an attempt to demonstrate that it is possible to continue the new model where the previous model ended.

The pinch-off criteria will be improved in future work. The idea is that when the bubble neck is small enough, the pinch-off process will be computed analytically using a separate asymptotic model. This will reduce numerical computational requirements due to meshing regions of relatively small length scales compared to the rest of the model. After pinch-off, the shape of the gas bubbles and the associated velocity and pressure fields near the pinch-off point will be used to reinitialize the numerical model and continue the simulation.

2.3 Governing Equations for the ALE Model

The incompressible Navier-Stokes and advection-diffusion equations are solved over each domain. Including the ALE moving mesh, there are five domains or application modes modeled in Comsol that are coupled with boundary conditions. The Boussinesq approximation is used to allow natural convection with the incompressible fluid model.

The ALE method only requires boundary conditions to be specified to link the liquid and vapor domains and account for vaporization.

This is different than having to formulate volume forces and sources as is required in a fixed-mesh method.

The first step in formulating these boundary conditions is to prescribe the mesh motion so that it follows the interface evolution. The mesh interface velocity is not the same as either the local vapor or liquid velocities since there is an influx/outflux of each relative to the interface, depending on if there is local vaporization or condensation. The mesh is allowed to slide tangentially along the interface to allow for improved mesh quality as deformation takes place, so only a normal component needs to be specified. The normal components are denoted with a subscript ‘n’. The normal vector convention is that the outward facing normal vector is positive, and each domain has its own outward normal. A diagram of the domain and normal vectors are shown in Figure 3. The normal velocity of the mesh is given by

$$u_{n,mesh} = \underline{u}_l \cdot \hat{\mathbf{n}}_l + v_{n,l} \quad (1)$$

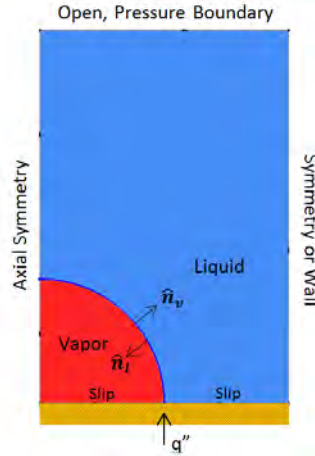


Figure 3. Liquid and Vapor domains with labeled boundary conditions and heat flux input at hot plate.

where $v_{n,l}$ is the relative normal liquid velocity to the interface, and it is calculated by taking the difference of heat flux on each side of the interface and using liquid and vapor enthalpies and densities in the calculation. The sign convention used assumes vaporization has a positive liquid velocity relative to the interface (i.e., liquid influx is positive). This calculation will be discussed in more detail later, after the thermal boundary conditions.

The next step is to couple the vapor and liquid domain velocities at the interface. The tangential components are equal, assuming a no-slip condition. The normal components differ by the sum of the magnitudes of the vapor and liquid velocities relative to the interface (i.e., the relative velocities are defined with the observer attached to the moving interface). These constraints, in terms of normal components, are shown in Eqn. 2 and 3.

$$(\underline{\mathbf{u}} - \underline{\mathbf{u}} \cdot \hat{\mathbf{n}})_l - (\underline{\mathbf{u}} - \underline{\mathbf{u}} \cdot \hat{\mathbf{n}})_v = 0 \quad (2)$$

$$(\underline{\mathbf{u}}_v \cdot \hat{\mathbf{n}}_v - \underline{\mathbf{u}}_l \cdot \hat{\mathbf{n}}_l) + v_{n,l} + v_{n,v} = 0 \quad (3)$$

The interface temperatures, in both the liquid and vapor domains, are set to the local saturation temperature as Dirichlet boundary conditions.

$$T_l = T_v = T_{sat} \quad (4)$$

With radiation neglected, the amount of heat going into vaporization is the sum of the conduction heat transfer into the inner and outer sides of the interface.

$$q''_{vaporization} = k_l \nabla T_l \cdot \hat{\mathbf{n}}_l + k_v \nabla T_v \cdot \hat{\mathbf{n}}_v \quad (5)$$

The relative or flux velocities can now be calculated using additional property data that can be temperature and pressure dependent. The property data can be represented with a curve-fit or table interpolation.

$$v_{n,l} = -\frac{q''_{vaporization}}{\rho_l(h_v - h_l)} \quad (6)$$

$$v_{n,v} = -\frac{q''_{vaporization}}{\rho_v(h_v - h_l)} \quad (7)$$

Vapor recoil may be included by adding the following terms to the stress boundary condition on the vapor domain along the interface. The boundary stress terms are separated into projected components to allow for incorporation into the weak form of the Navier-Stokes equations in Comsol Multiphysics. The velocities in Eqn. 8 are relative to the interface.

$$\begin{bmatrix} P_x \\ P_y \\ P_z \end{bmatrix}_{recoil} = \rho_l (\underline{\mathbf{u}}_l \cdot \hat{\mathbf{n}}_l) \underline{\mathbf{u}}_l - \rho_v (\underline{\mathbf{u}}_v \cdot \hat{\mathbf{n}}_v) \underline{\mathbf{u}}_v \quad (8)$$

The normal-stress boundary condition on the liquid-gas interface is

$$(\underline{\underline{\sigma}}_l - \underline{\underline{\sigma}}_g) \hat{\mathbf{n}} = \sigma \kappa \hat{\mathbf{n}} + P_{recoil}, \quad (9)$$

where $\underline{\underline{\sigma}}_{g,l}$ are the stress tensors for the gas and the liquid, defined as

$$\underline{\underline{\sigma}}_{g,l} = \left[-P \underline{\underline{I}} + \eta (\nabla \underline{\mathbf{u}} + (\nabla \underline{\mathbf{u}})^T) \right]_{g,l} \quad (10)$$

$\hat{\mathbf{n}}$ is the outward unit normal to the gas-liquid interface, σ is the surface tension of the interface, and κ is the curvature of the interface defined as

$$\kappa = \nabla_s \cdot \hat{\mathbf{n}}, \quad (11)$$

where ∇_s is the surface divergence operator. The Navier-Stokes equations on the sub-domains remain unchanged since the surface tension is implemented as a boundary condition.

Multiplying both sides of Eqn. 9 by a test function and integrating results in,

$$\begin{aligned} \int_{\partial\Omega} (\tilde{\varphi} \underline{\underline{\sigma}}_l \hat{\mathbf{n}}) dA &= \int_{\partial\Omega} (\tilde{\varphi} \underline{\underline{\sigma}}_g \hat{\mathbf{n}}) dA \\ &\quad + \int_{\partial\Omega} (\tilde{\varphi} \sigma \kappa \hat{\mathbf{n}}) dA. \end{aligned} \quad (12)$$

Applying the surface divergence theorem [2] to the last surface integral on the right-hand side and substituting back in yields,

$$\begin{aligned} \int_{\partial\Omega} (\tilde{\varphi} \underline{\underline{\sigma}}_l \hat{\mathbf{n}}) dA &= \int_{\partial\Omega} (\tilde{\varphi} \underline{\underline{\sigma}}_g \hat{\mathbf{n}}) dA \\ &\quad - \int_{\partial\Omega} (\sigma \nabla_s \tilde{\varphi}) dA \\ &\quad + \int_{\partial^2\Omega} (\sigma \tilde{\varphi} \hat{\mathbf{m}}) ds, \end{aligned} \quad (13)$$

where $\hat{\mathbf{m}}$ is a unit binormal vector at the contact line, and $\tilde{\varphi}$ is a test function.

This last equation can be applied as boundary and point weak expressions in Comsol. This applies to 2D, 2D axisymmetric, and 3D models, although some minor modifications need to be made to express this in polar coordinates.

2.4 Governing Equations for the Level-set Model

The finite element level-set model incorporates phase change in a method similar to Son and Dhir [3,4], except that a ghost fluid method cannot be implemented in Comsol Multiphysics for calculating heat fluxes on the interface. To

account for phase change, terms are added to the continuity and energy equations only on the interface using a delta function. Vapor recoil is accounted for, similarly, by adding a term to the momentum equation, again only on the interface using a delta function. The temperature recovery method described in [5] is used to maintain the saturation temperature on the interface, where the level-set variable is 0.5. Comsol Multiphysics uses a level-set variable that varies between 0 and 1, as opposed to -1 to 1. The first use, to the best knowledge of the author, of the temperature recovery method appears in [6]. The temperature recovery method works by proportionally increasing the mass vaporization (condensation) rate as the local interface temperature deviates from the saturation temperature. This is solved at each time step inside the Comsol solver along with the velocity, temperature, and level-set fields. In effect, the temperature recovery method determines the amount of fluid vaporization (condensation) required to maintain the interface temperature, rather than calculating the mass vaporization (condensation) rate directly from the temperature gradients on each side of the interface, since these gradients are not available and not accurately computed without using a ghost fluid method. The mass vaporization (condensation) rate calculated from heat fluxes at the interface should, in theory, dictate enough vaporization (condensation) to keep the interface at saturation temperature. With this in mind, determining the mass vaporization (condensation) rate to some value that is enough to maintain the interface temperature at saturation should lead to the same result. The temperature recovery method has been verified to maintain interface temperatures within approximately 0.3 °C. The finite element model utilizes quadratic triangular (tetrahedral for 3D) Lagrange elements for the fluid, thermal, and level-set equations. The present model does not account for thin film (micro-scale) boiling, but a lubrication model can be added in Comsol Multiphysics and coupled to the current model.

Aside from the temperature recovery method for determining the mass vaporization (condensation) rate, the formulation is very similar to Son and Dhir's method [3], which is as follows.

First, the mass vaporization (condensation) rate is determined from the interface temperature profile, shown in Eqn. 14. Note that \dot{m} is per unit interface surface area. The proportionality constant 'C' can be adjusted if the vaporization (condensation) rate is insufficient to maintain saturation temperature on the interface. Setting this constant too large will lead to numerical instabilities.

$$\dot{m} = C \rho_l \left(\frac{T - T_{sat}}{T_{sat}} \right) \quad (14)$$

Also, the mass vaporization (condensation) rate can be formulated as an interfacial normal flux, which is used for the continuity source term on the interface,

$$\dot{m} = \rho_f (\underline{\mathbf{U}} - \underline{\mathbf{u}}_f) \cdot \hat{\mathbf{n}} \quad (15)$$

where \mathbf{U} is the interface velocity and the subscript 'f' indicates the fluid, which could be liquid or vapor. The next step is to evaluate Eqn. 15 for both the liquid and vapor, and then rearrange for the liquid and vapor velocities. Equations 16 and 17 represent the normal components only – vector notation is omitted for clarity.

$$u_l = U - \frac{1}{\rho_l} \dot{m} \quad (16)$$

$$u_v = U - \frac{1}{\rho_v} \dot{m} \quad (17)$$

Taking the difference in the liquid and vapor velocities at the interface provides the divergence created by the phase-change and corresponding change in density. The fluid is treated as incompressible everywhere in the fluid, except on the interface region, and the continuity source term is Eqn. 18 multiplied by an interface delta function that only allows the source term to be non-zero on the interface.

$$\underline{\mathbf{u}}_l - \underline{\mathbf{u}}_v = \left(\frac{1}{\rho_v} - \frac{1}{\rho_l} \right) \dot{m} \hat{\mathbf{n}} \quad (18)$$

The continuity equation with the additional source term is shown in Eqn. 19 and 20, where δ is the interface delta function.

$$\nabla \cdot \underline{\mathbf{u}} = \delta (\underline{\mathbf{u}}_l - \underline{\mathbf{u}}_v) \quad (19)$$

$$\nabla \cdot \underline{\mathbf{u}} = \delta \left(\frac{1}{\rho_v} - \frac{1}{\rho_l} \right) \dot{m} \hat{\mathbf{n}} \quad (20)$$

The tangential stress on the vapor and liquid sides of the interface are equal while there is a

jump condition in the normal stress. The normal stress changes across the interface because of the effects of surface tension and vapor recoil. Eqn. 21 prescribes that the tangential stress on each side of the interface is equal. Eqn. 22 is the normal stress jump condition.

$$\hat{\mathbf{n}} \cdot [\mu_l(\nabla \underline{\mathbf{u}} + \nabla \underline{\mathbf{u}}^T)_l - \mu_v(\nabla \underline{\mathbf{u}} + \nabla \underline{\mathbf{u}}^T)_v] \times \hat{\mathbf{n}} = 0 \quad (21)$$

$$\begin{aligned} -p_l + p_v + \hat{\mathbf{n}} \cdot [\mu_l(\nabla \underline{\mathbf{u}} + \nabla \underline{\mathbf{u}}^T)_l \\ - \mu_v(\nabla \underline{\mathbf{u}} + \nabla \underline{\mathbf{u}}^T)_v] \cdot \hat{\mathbf{n}} \\ = \sigma\kappa - \left(\frac{1}{\rho_v} - \frac{1}{\rho_l}\right)\dot{m}^2 \end{aligned} \quad (22)$$

The forces from surface tension and vapor recoil are added to only the interface region as volume force terms using the interface delta function.

The next step is to account for the latent heat of vaporization in the energy equation. This is done by adding a term, multiplied by the interface delta function, to account for the energy liberated (absorbed) by condensation (vaporization). The modified energy equation is shown in Eqn. 23, where h_{lv} is the latent heat of vaporization.

$$\rho_f c_f \left(\frac{\partial T_f}{\partial t} + \underline{\mathbf{u}}_f \cdot \nabla T_f \right) = \nabla \cdot k_f (\nabla T)_f - \delta \dot{m} h_{lv} \quad (23)$$

The level-set function is updated since it only accounts for advection of the interface by default – it does not account for interface movement as vapor phase is generated. The modified level-set function is shown in Eqn. 24.

$$\frac{\partial \phi}{\partial t} + \underline{\mathbf{U}} \cdot \nabla \phi = 0 \quad (24)$$

where,

$$\underline{\mathbf{U}} = \underline{\mathbf{u}}_f + \frac{\dot{m}}{\rho_f} \hat{\mathbf{n}} \quad (25)$$

This completes the necessary modifications to the finite-element level-set model, and it now accounts for vaporization and condensation.

3. Results and Discussion

The single-bubble models use an initial bubble radius of 3 mm. The surface tension coefficient

is 0.07 N/m for all models. Pressure and gravity are 1 atm and 9.81 m/s², respectively.

3.1 ALE Results

The heat flux input over the heater surface exposed to liquid is 20 W/cm² and the region of the heater surface underneath the vapor bubble is 0.2 W/cm². The exterior contact angle is 55 degrees. The heat flux is ramped in over 0.1 s. The model is axisymmetric. Figure 4 shows the temperature distribution with velocity arrows over-plotted and the interface marked with a white line at selected time steps.

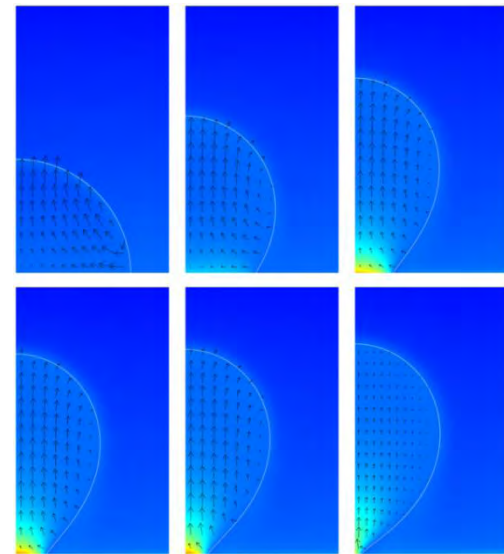


Figure 4. ALE simulation results for a contact angle of 55 degrees.

The vapor in the bubble reaches relatively high temperatures even at low heat fluxes. The model was run with 0.2 W/cm² input under the vapor bubble to reduce the peak temperatures in the vapor domain, which were observed to be in excess of 1000 K at higher heat fluxes. The reduced heat flux under the vapor bubble limits peak vapor temperatures to approximately 450 K. The next step is to include another heat transfer domain to incorporate the solid heater plate. This will allow for a physical determination of the appropriate heat distribution under the vapor bubble and the rest of the heater surface exposed to liquid. The liquid and vapor have significantly different thermal conductivities, so the heat flux is not expected to be uniform over the entire heater. However, the

heater plate will physically smooth out temperature gradients along the surface of the heater and between the vapor and liquid. This is expected because of the higher thermal conductivity in the solid heater plate compared to water in both liquid and vapor states.

The ALE method can also model a pinned contact line with phase-change. Figure 5 shows the results from the pinned contact-line model.

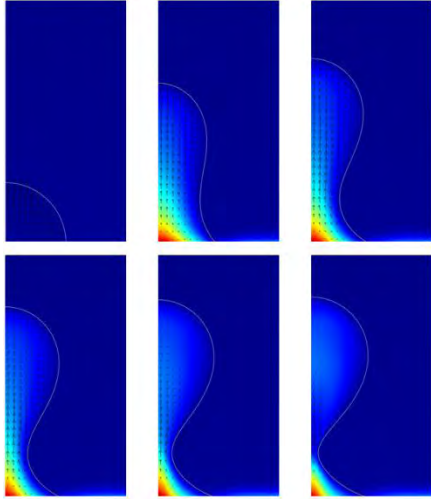


Figure 5. ALE results for a pinned contact line.

The non-isothermal ALE model requires more remeshing to reach pinch-off than the previous isothermal model [7]. This appears to be primarily due to the addition of vaporization and condensation on the interface. The pinch-off process was not successful due to the solver being unable to restart with the current approximated solution on the new geometry after pinch-off. This is likely to be because the approximated solution created did not satisfy the model constraints and boundary conditions within solver tolerances. The intermediate model proposed would provide a more accurate solution to resume the model after pinch-off. It is expected that this would be successful in continuing the model after pinch-off.

3.2 Level-Set Results

The heat flux input over the entire surface of the hot plate is 15 W/cm^2 . The exterior contact angle is 55 degrees, and the hot surface enforces a slip length condition. The model was performed in 3D and utilized symmetry

conditions to minimize the computational domain. A $1/8^{\text{th}}$ vertical wedge was modeled. This provides similar results to the axisymmetric case in the ALE model. The mesh resolution is relatively coarse in the level-set model to reduce computational expense. This is likely to make the solution mesh-dependent, especially near the contact line. The results in Figure 6 show the iso-surfaces of the level-set function values of 0.5. The heat flux input is started immediately, without ramping in. The liquid is sub-cooled by 5K at the upper tank boundary, and the initial temperature condition is a linear profile from saturation temperature at the hot surface to the sub-cooled temperature at the upper tank boundary.



Figure 6. 3D, $1/8$ -symmetry model of a single vapor bubble.

The level-set model can be extended to multiple vapor bubbles. The next results shown in Figure 7 were performed in 2D to minimize computational expense. While the 2D model neglects the second curvature used for calculating pressure due to surface tension, it does provide qualitative results for the behavior of the interactions between bubble interactions and departure frequency.

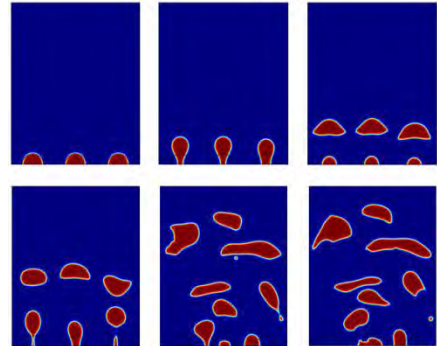


Figure 7. 2D simulation of three nucleation sites.

The level-set reinitialization parameter needs to be chosen carefully since the default value in Comsol Multiphysics 4.2 tends to introduce a significant amount of interface movement due to accumulation of error in the reinitialization procedure that occurs at each time step. The value of the reinitialization parameter is specific to each problem. It has been found that values on the order of 0.01 or less provide the best results. The amount of error accumulation was determined by running level-set models with a geometry undergoing rigid body rotation and/or translation. The rigid body movement was achieved by prescribing a velocity field that forced rigid body rotation or a uniform velocity field to provide rigid body translation. With the rigid body motion prescribed, the only source of deformation from the original geometry is from error accumulation due to the reinitialization of the level-set function at each time step.

4. Conclusions

The ALE model needs more refinement to allow for a successful pinch-off procedure. It is likely that the approximated solution, for restarting the model with the post-pinch-off geometry, does not satisfy model constraints within the solver tolerances. The approximate solution attempted here was made by taking the solution at the last time step before pinch-off and performing local modifications to approximate the solution a small finite time after the initiation of pinch-off. This worked in the previous model [7], but this model has a key difference of having discontinuous velocity fields. There is a jump in velocity at the interface due to phase change, so mapping the solution to the new geometry is more difficult. It is expected that including an intermediate pinch-off model will provide a more accurate solution and alleviate the inconsistent initial solution problem when resuming the model.

The ALE model allows for more control over the contact line dynamics. A contact line mobility and hysteresis model can be included to determine the transition from pinned to dynamic contact line movement. The level-set model allows for boundary conditions to be modified at the weak level in Comsol Multiphysics, but since the interface is smeared over a distance on the

order of one mesh element length, the control over the contact line is less precise.

The ALE method allows for a more physical approach for determining the rate of vaporization (condensation) at the liquid-vapor interface and for more detail of the contact line dynamics. However, when it comes to modeling more complicated heater surfaces or interactions of multiple vapor bubbles, the level-set model is more practical. The level-set model complements the ALE model, and by using both, modeling of the finer detail of the dynamics of a single bubble and interactions of many vapor bubbles and nucleation sites on more complicated geometry is possible.

5. References

1. Incropera, F. P., & DeWitt, D. P. (2002). Introduction to heat transfer. (4th ed., pp. 558-563). New York: John Wiley & Sons.
2. C.E. Weatherburn, Differential Geometry of Three Dimensions, 238-242, University Press, Cambridge (1955).
3. Son, G. & Dhir, V. K. (2007). A level set method for analysis of film boiling on an immersed solid surface. *Numerical Heat Transfer: Part B*, (52), 153-177.
4. Son, G. & Dhir, V. K. (2008). Numerical simulation of nucleate boiling on a horizontal surface at high heat fluxes. *International Journal of Heat and Mass Transfer*, (51), 2566-2582.
5. Tsujimoto, K. , Kambayashi, Y. , Shakouchi, T. & Ando, T. (2009). Numerical simulation of gas-liquid two-phase flow with phase change using cahn-hilliard equation. *Turbulence, Heat and Mass Transfer*, 6, 1-12.
6. T. Kunugi, N Saito, Y. Fujita and A. Serizawa. Direct Numerical Simulation of Pool and Forced Convective Flow Boiling Phenomena, *Heat Transfer* 2002, 3:497-502, 2002
7. Christopher J. Forster and Marc K. Smith, The Transient Modeling of Bubble Pinch-Off Using an ALE Moving Mesh, *Comsol* (2010)